Research Article

Comparison of glioma stem cells to neural stem cells from the adult human brain identifies dysregulated Wnt- signaling and a fingerprint associated with clinical outcome ☆

Cecilie Jonsgar Sandberg[a,b,]*, Gabriel Altschuler[d], Jieun Jeong[d], Kirsten Kierulf Strømme[a], Biljana Stangeland[a], Wayne Murrell[a], Unn-Hilde Grasmo-Wendler[c], Ola Myklebost[c], Eirik Helseth[b], Einar Osland Vik-Mo[a,b], Winston Hide[d,1], Iver A. Langmoen[a,b,1]

[a]Vilhelm Magnus Laboratory, Institute for Surgical Research, University of Oslo, Norway
[b]Departments of Neurosurgery, Oslo University Hospital, Oslo, Norway
[c]Tumor Biology, Oslo University Hospital, Oslo, Norway
[d]Department of Biostatistics, Harvard School of Public Health, Boston, MA, USA

ARTICLE INFORMATION

ABSTRACT

Glioblastoma is the most common brain tumor. Median survival in unselected patients is <10 months. The tumor harbors stem-like cells that self-renew and propagate upon serial transplantation in mice, although the clinical relevance of these cells has not been well documented. We have performed the first genome-wide analysis that directly relates the gene expression profile of nine enriched populations of glioblastoma stem cells (GSCs) to five identically isolated and cultivated populations of stem cells from the normal adult human brain. Although the two cell types share common stem- and lineage-related markers, GSCs show a more heterogeneous gene expression. We identified a number of pathways that are dysregulated in GSCs. A subset of these pathways has previously been identified in leukemic stem cells, suggesting that cancer stem cells of different origin may have common features. Genes upregulated in GSCs were also highly expressed in embryonic and induced pluripotent stem cells. We found that canonical Wnt-signaling plays an important role in GSCs, but not in adult human neural stem cells. As well we identified a 30-gene signature highly overexpressed in GSCs. The expression of these signature genes correlates with clinical outcome and demonstrates the clinical relevance of GSCs.

© 2013 The Authors. Published by Elsevier Inc. All rights reserved.

*Corresponding author at: Institute for Surgical Research, Oslo University, 0405 Oslo, Norway. Fax: +47 23071398.
    E-mail address: cesandbe@medisin.uio.no (C.J. Sandberg).
    [1] Contributed equally to this work.

Introduction

The cancer stem cell hypothesis proposes that the cells of cancers are organized in hierarchies initiated and maintained by a cancer stem cell (CSC). The existence of such a hierarchy in tumor propagation was first described in hematopoietic malignancies [3,28], but has later been extended to a variety of other cancers. The strongest support for this model comes from transplantation assays in immunodeficient mice where only a subpopulation of the cells in the tumor bulk can initiate and maintain the tumor upon serial grafting. Despite substantial evidence from preclinical studies, the relevance of this model to human disease is uncertain. Two studies have now identified a leukemic stem cell (LSC) signature of gene expression associated with acute myeloid leukemia and it has shown that this signature correlates with the clinical outcome [9,13]. These studies have established LSCs as significant in clinical disease. A direct comparison of the gene expression profiles of LSCs and hematopoietic stem cells (HSCs) grown under identical conditions, has resulted in new insight into critical pathways regulating CSCs in leukemia [33].

Besides a paucity of clinical evidence, testing the cancer stem cell model is challenging due to the lack of markers that consistently define CSCs. For example, LSCs were initially believed to be restricted to the CD34+ CD38- population, but have later been shown to be present in both the CD34- and CD34+CD38+ populations [9,47,48]. Such heterogeneity has also been shown in solid cancers. In glioblastoma (GBM), the best characterized surface marker is CD133 (prominin-1), but CD133⁻ cells also initiate tumors upon xenografting [42,52] and it has been suggested that the true GBM stem cell (GSC) resides in the CD133⁻ population [6]. Thus, surface marker-sorted CSC populations cannot be universally defined and functional confirmation of CSC activity using well-validated tumor initiation assays is required.

GBM is both the most common and the most malignant brain tumor. It is invariably lethal with a median survival of less than 10 months in unselected patient populations [18]. The existence of CSCs in brain tumors was first suggested following the isolation of clonogenic stem cell-like spheres from human GBM tissue [21]. Serum-free, growth factor-enriched culturing conditions, developed to isolate and expand somatic neural stem cells [44], have been shown to be a robust method for enrichment of stem-like cells from a range of organs and malignancies [43]. Here, we have used this technique to directly compare GSCs to ahNSCs harvested from the subventricular zone. ahNSCs can differentiate into the three neural lineages [22], including functional neurons [34] that develop synaptic networks [34,35]. Tumor biopsies cultured under identical conditions maintain genotype, phenotype and the ability to form invasive tumors [10,29,51]. Sphere growth rate and the ability to form spheres under these conditions is related to tumor grade [49] and is an independent prognostic factor within the glioblastoma group [27].

Global gene expression studies of GSC populations have led to the identification of subgroups [17,32] but have not identified which pathways regulate cancer stem cell functions and do not address the question of how to specifically target GSCs. Here we directly compare the gene expression from functionally validated, enriched fractions of CSCs from a solid tumor to its closest functional non-tumorigenic, adult cell population. We identify the genes, pathways and networks shared between ahNSCs and GSCs, and those specific to the oncogenic phenotype of GSCs. We highlight significant differences found in the expression of classical stem cell signaling pathways, in particular dysregulation of the Wnt-pathway through SFRP1, a Wnt-signaling inhibitor downregulated in GSCs. Cancer stem cell-specific genes have been validated and we show that their expression predicts clinical outcome in GBM patients.

Materials and methods

Fresh human biopsy specimens and spheroid cultures

Biopsy specimens were obtained from informed and consenting patients, and the tissue harvesting was approved by the Norwegian National Committee for Medical Research Ethics. Histopathological diagnosis and grading were performed by neuropathologists according to the World Health organization classification [25]. ahNSC cultures were established from ventricular wall biopsies of 5 patients operated on for medically intractable temporal lobe epilepsy (mean age 42, range 33–60). GSC cultures were established from tumor biopsies from nine patients with histopathologically verified glioblastoma (mean age 61, range 48–71). The cells were isolated mechanically and enzymatically and further cultured in serum free medium enriching for stem cells as described earlier [51]. For dissociation of brain tissue into single cells, Trypsin-EDTA was substituted by papain (Worthington Biochemical Corporation).

RNA isolation

Total RNA from spheres was isolated using Qiazol and the RNeasy Micro Kit (Qiagen GmbH, Hilden, Germany). The concentration of each RNA sample was determined by using a Nanodrop spectrophotometer and analyzed for quality using an Agilent 2100 Bioanalyzer with the RNA Nano Assay. Only RNA samples with a RIN value >8 were included for further analysis.

Microarray hybridization and analysis of microarray data

RNA of each sample was reverse transcribed and amplified using the NanoAmp RT-IVT Labeling Kit (Applied Biosystems). The resulting cRNA (10 µg) was fragmented and hybridized to Applied Biosystems Human Genome Survey Microarray V2.0 (Applied Biosystems) according to the manufacturer's protocol Analysis and statistics were done using J-Express (Molmine), R (version 2.11.1) and Bioconductor. External data files were extracted from the GEO database. For details regarding bioinformatic analysis see supplemental information.

Quantitative real-time PCR

Total RNA was reverse transcribed using the High Capacity cDNA synthesis kit (Qiagen, Germany) and followed by qPCR using predesigned TaqMan gene expression assays and reagents (Applied Biosystems). Both the standard curve method and the $2^{-\Delta\Delta CT}$ method were used to analyze the data. For details regarding TaqMan gene expression assays see supplementary information and supplementary Table S7.

Immunofluorescence

Spheres and tumor tissue were fixed in paraformaldehyde, cryoprotected and incubated in OCT (Tissue-TEK, Sakura Finetek, CA). Blocks were then cryosectioned at 10 or 20 μm on a freezing microtome, and thawed onto Super Frost/Plus microscope slides (Menzel-Gläzer, Braunschweig, Germany). Sections were washed, blocked and incubated in primary antibody overnight at 4° C. Analysis and image acquisition was done on an Olympus BV 61 FluoView confocal microscope (Olympus, Hamburg, Germany), using the FV10-ASW 1.7 software (Olympus). For details regarding antibodies see supplementary information.

Western-blot analysis

Cells were lysed in preheated (100 °C) buffer, then boiled, sonicated and centrifuged to remove unsolubilized protein. Aliquots of 30 ug were denatured and separated on SDS gradient gels and transferred to PVDF membranes. Membranes were incubated with blocking buffer, washed and incubated with primary antibody in blocking buffer at 4 °C overnight. The membranes were further incubated with HRP-conjugated secondary antibodies and quantified using ECL Advance Western blotting detection solution (Amersham) and the Kodak Image Station 400 MM PRP (Kodak). For details regarding antibodies see supplementary information.

SFRP1 stimulation

GSCs and ahNSCs were passaged into single cells and seeded in 96 well plates (Sarstedt AG & Co, Germany) at a density of 500 cells per well in stem cell enriching media. SFRP1 was added daily in three different concentrations (100, 400, and 800 ng/ml) for 2 weeks. Each assay included 6 replicates of each treatment and was repeated 3 times in total. Spheres in individual wells were inspected and counted manually using a microscope and an automatic colony counter (Gelcount, Oxford Optronix). Cell proliferation was measured as change in total level of nucleic acids as compared to untreated control cells using CyQUANT according to the manufacturer's instructions (Molecular Probes, Invitrogen).

Accession Numbers

Microarray data have been submitted to the Gene Expression Omnibus (GSE31262) and the online resource "The Stem Cell Discovery Engine" [19].

Results

Obtaining and characterizing samples

ahNSCs and GSCs were cultivated as free floating spheres from five normal subventricular zone and nine primary GBM tissue biopsies, respectively. All cell cultures formed secondary spheres. Both ahNSCs and GSCs maintained the ability to proliferate, self-renew and differentiate in vitro, but only the GSCs gave rise to tumors upon orthotopic transplantation to SCID-mice [49]. GSCs were able to initiate tumor formation upon serial transplantation, and maintained their genome, global expression profile and ability to differentiate after in vitro cultivation [51]. All but one GBM tissue sample (G3) was IDH1 mutation negative in line with the frequency of IDH1 mutations in primary GBMs [24].

GSCs are more heterogeneous than ahNSCs and represent different subtypes of GBMs

Hierarchical clustering based on the pair-wise correlation of global gene expression profiles separated the GSC and ahNSC samples, indicating that the transcriptional programs of individual GSC cultures differ from ahNSCs (Fig. 1A). There was generally a much greater heterogeneity across the GSCs than across the ahNSCs (0.81 vs. 0.47; average square of differences to the mean per probe). Two outliers were identified in the tumor group (G2 and G3) (Fig. 1C & D). Of these, G3 showed a pronounced difference in behavior compared to the other GSC cultures. In addition to a more limited differentiation ability in vitro, it also formed a compact noninvasive tumor bulk containing spindle-like cells when transplanted to SCID mice [51]. Since G3 obviously had lost its ability to mimic the invasive nature of GBMs, it was excluded from further gene-expression analysis.

Investigation of GBM heterogeneity in tissue biopsies suggests the existence of molecular subgroups [12,40,50]. The Cancer Genome Atlas (TCGA), being the most significant study, describes four such subgroups of GBMs: the proneural, neural, classical and mesenchymal subtype. The subtypes are identified dependent on the level of enrichment of a total of 840 genes (210 genes per class). To explore if such subtypes were present among our population of GSCs, we calculated the enrichment of these subtypes individually for every sample. The expression score was calculated as the mean expression of the genes in the signature using the rank-normalized gene expression scores (z-score). 173 samples from the original TCGA-study were included as positive controls. While all ahNSCs showed a homogeneous correlation with the neural subtype, seven of the GSC cultures were enriched in genes representing either the classical, proneural or mesenchymal subtype. Two of the GSC cultures (including the outlier G3) did not show enrichment of any particular subgroup (supplementary Fig. S1 and supplementary Table S1). We further classified our samples according to the less well established GSC classification by Lottaz et al. [32]. This classification contains only two groups, (1) mesenchymal and (2) proneural. Hierarchical clustering according to their 24-gene signature identified one sample as belonging to their type 1 (G9) while the other 7 belonged to type 2 (Supplementary Fig. S1). The outlier (G3) clustered separately from the others and was generally much less enriched in signature genes.

GSCs and ahNSCs share common stem- and lineage-related markers

To determine the common molecular phenotype of ahNSCs and GSCs, we directly compared the expression of known "stemness" genes as well as markers of the three principal cellular components of the nervous system - neurons (DCX, NCAM1, TUBB3, and MAP2), astrocytes (CD44, VIM, GFAP, and SLC1A3) and oligodendrocytes (OLIG2, CNP, CA2, and CSPG4). GSCs and ahNSCs expressed approximately the same levels of stemness markers, such as nestin (NES), SSEA1 (FUT4), OCT4 (POU5F1), BMI1 (PCGF4), β1-integrin (ITGB1) and SOX2. There was no significant difference in the expression of markers for neurons, astrocytes and oligodendrocytes (Fig. 2A). CD133 (PROM1) and MELK were
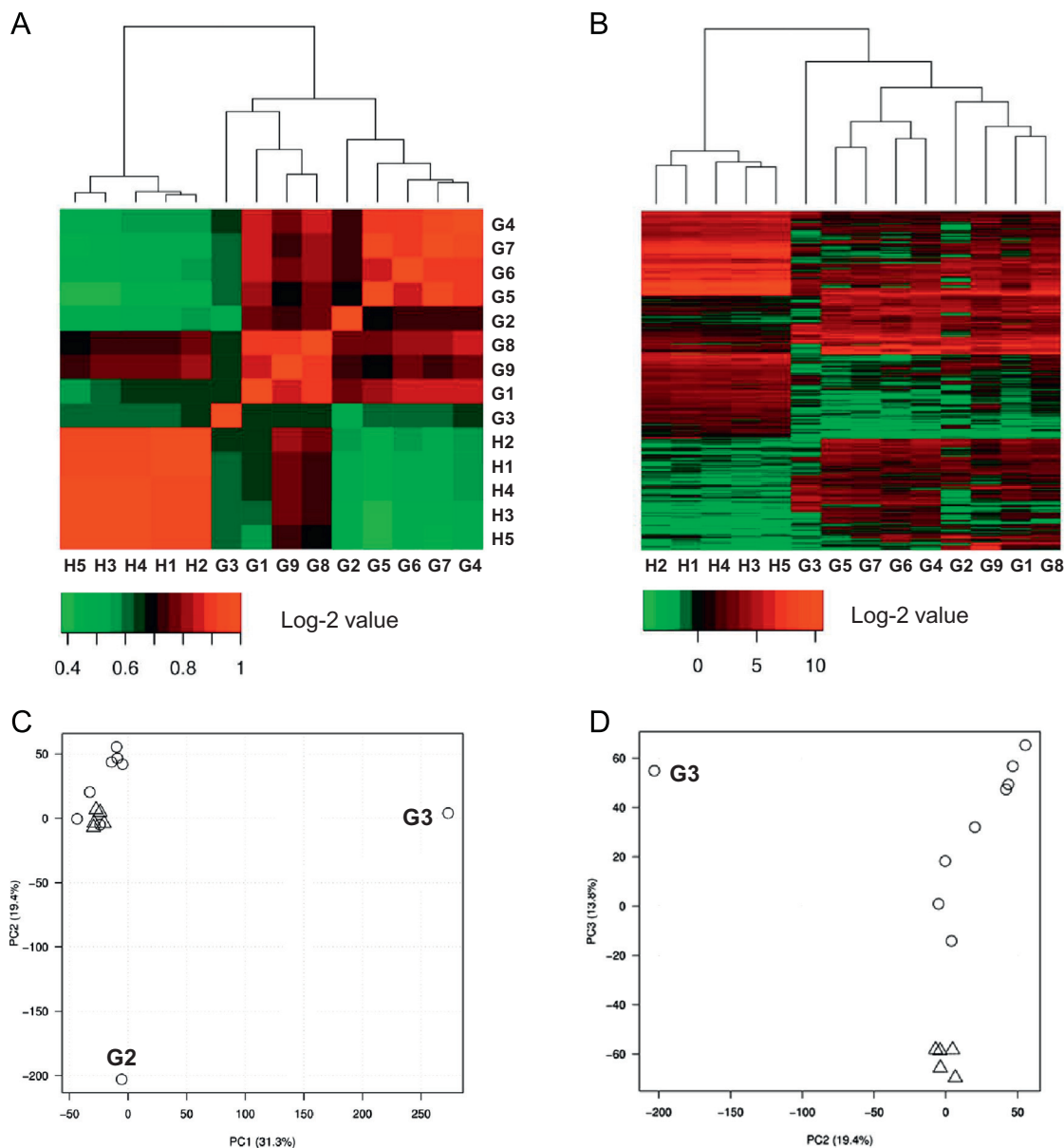
Q3 Fig. 1 – Gene expression profiles of GSCs and ahNSCs identify differentially regulated transcriptomes: (A) Unsupervised hierarchical clustering analysis completely separates GSCs and ahNSCs. (B) Unsupervised hierarchical clustering analysis of the most significantly regulated genes identified by the Rank Product Algorithm (1% false discovery rate). (C) Principal Component Analysis of GSCs (○) and ahNSCs (△). The first and second principal components identified G2 and G3 as outliers. (D) Principal Component Analysis of GSCs (○) and ahNSCs (△). The second and third principal components distinguished ahNSCs and GSCs.

significantly upregulated in GSCs (Fig. 2A). Using immunofluorescence we investigated the expression of selected markers (NES, GFAP, MELK, CXCR4, BMI1 and SOX2) at the protein level. All markers were similarly expressed, except for SOX2 which was overexpressed in GSCs (Fig. 2B).

A GSC expression index correlates with patient survival

Recently, it was shown for the first time that an LSC gene signature predicts patient survival in human leukemia [9,14], providing the impetus for an analogous investigation in GBM. Using the Rank Product algorithm [5] at a stringent threshold (0.1% false discovery rate (FDR)), we identified 179 genes being

significantly upregulated in GSCs compared to ahNSCs. An additional filter was applied (fold change > 5; coefficient of variation < 30 in GSC samples; average log2 < 1 for ahNSCs) to isolate a 30-gene signature which was highly overexpressed in all GSC samples studied (Fig. 3A and Table S2). This GSC signature included MELK, a gene known to regulate self-renewal and proliferation of both neural stem cells and GSCs in vitro and in vivo [37,38]. Interestingly, a literature search for each signature gene identified eleven of these as downstream targets of or related to the Notch-, Hedgehog- or Wnt- pathways (Table S2). The signature was further projected onto a network of protein association data, including protein interactions, co-expression, co-localization and domain similarity [53] (Fig. 3B). The network
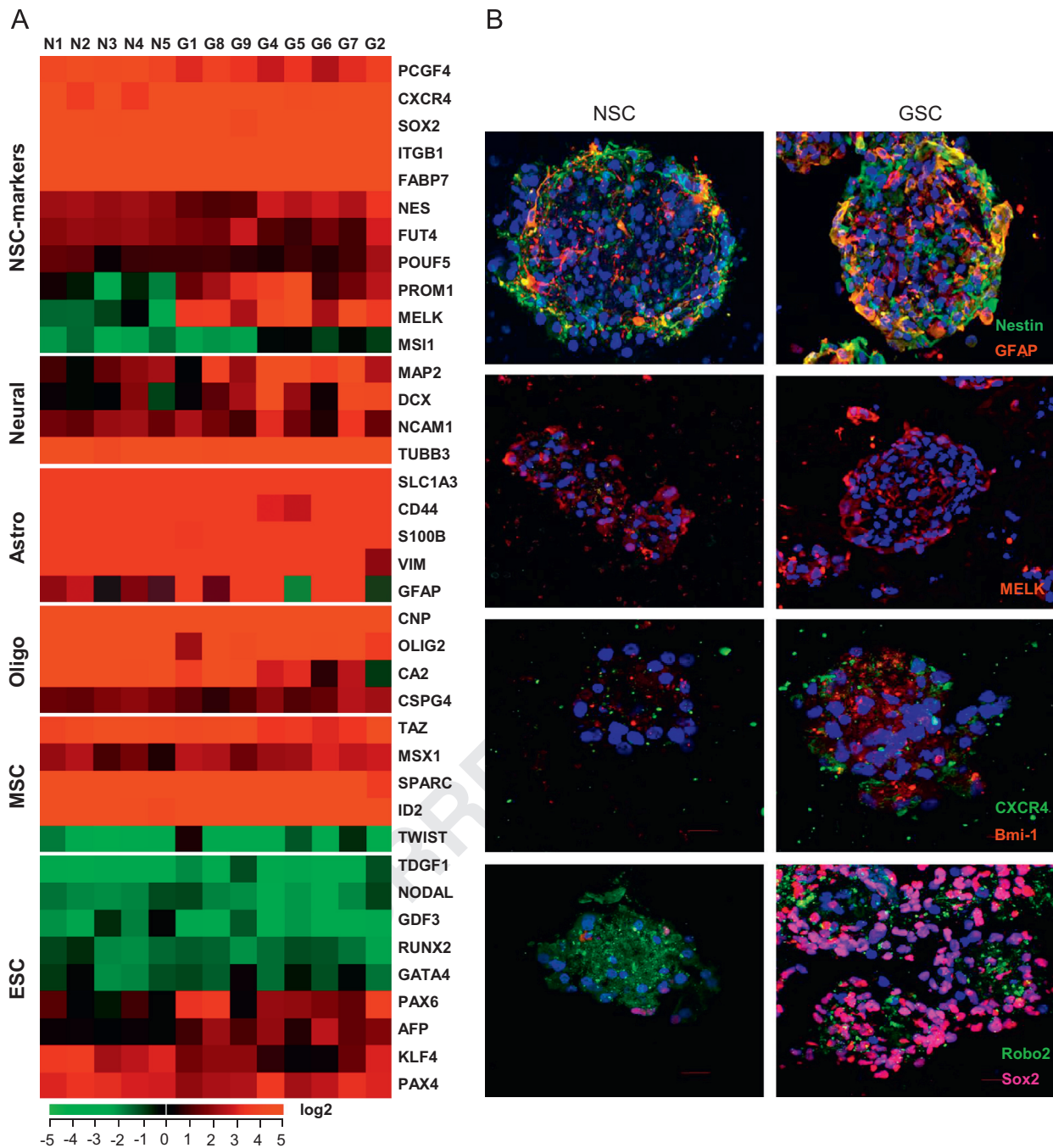
Fig. 2 – Expression of stem cell- and lineage-markers in ahNSCs and GSCs: (A) Gene expression levels of markers related to neural stem cells, neural lineages (neurons, astrocytes, oligodendrocytes), mesenchymal stem cells (MSCs) and embryonal stem cells (ESCs). The individual panels were made using one-dimensional clustering analysis of genes. (B) Immunofluorescence of selected markers in spheres. Left-side panel shows expression in ahNSCs while right panel shows expression in GSCs. Cell nuclei were stained with Hoechst (blue).

analysis demonstrated that a high proportion of the signature genes codes for proteins that are known to physically interact with each other, strongly suggesting that these play a coordinated role in the regulation on GSCs. Their enriched set of biological processes involve proliferation and cell-division (gene ontology analysis, Table S2).

We calculated a GSC expression index for each array from a publically available dataset containing gene expression levels for normal brain tissue, and low- and high grade gliomas [45], based on the summed Z-scores of the 30 genes in the GSC signature. This index correlated to an increasing grade of malignancy (Fig. 3C and Table S3).

The value of this index in predicting clinical outcome was assessed using two additional publicly available gene expression data-sets of high-grade gliomas [12,40]. In each study, patients were stratified into two groups according to the expression of the
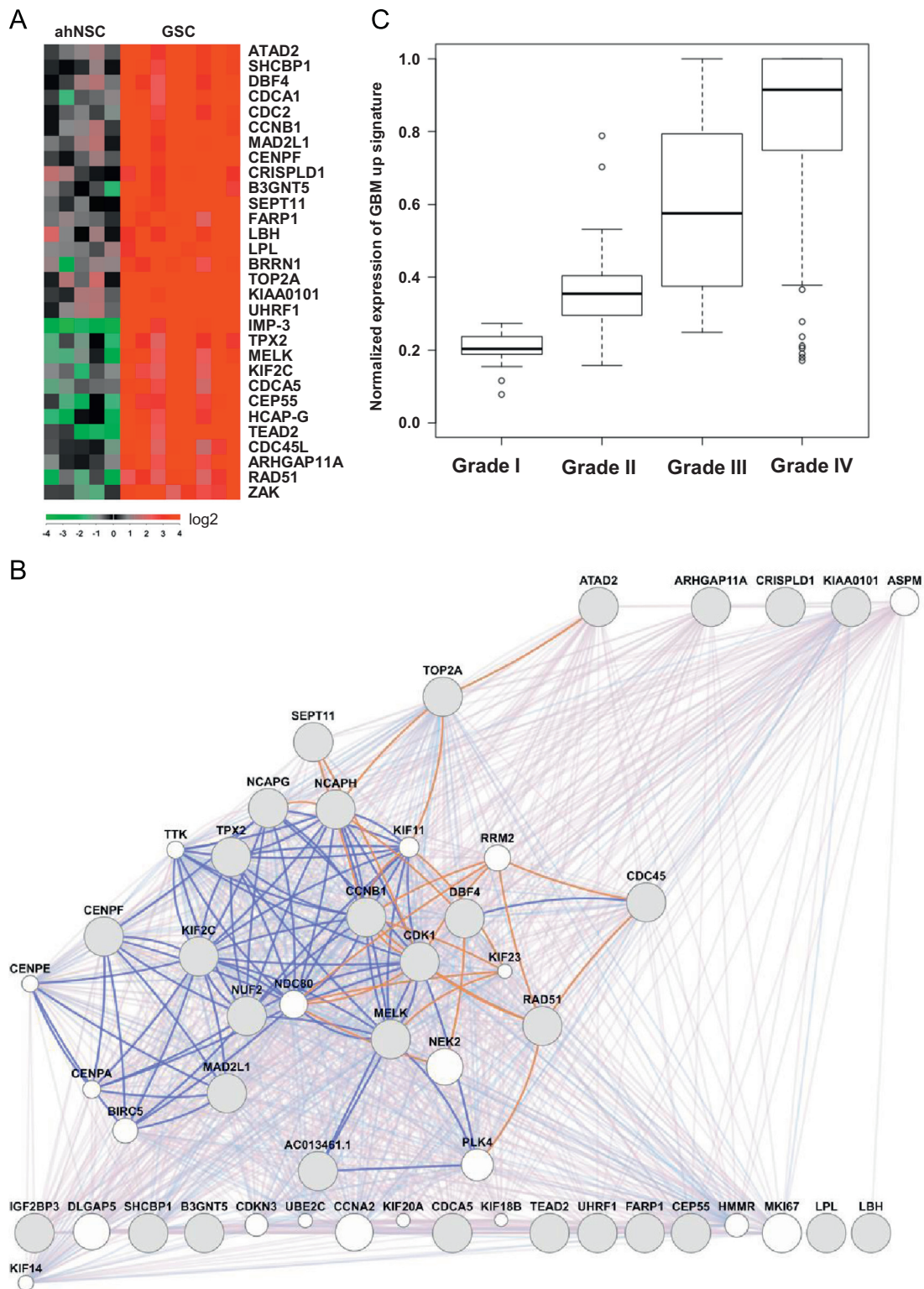
Fig. 3 – A gene signature of GSC-upregulated genes correlates with histology of glioma patients: (A) Heatmap of the expression of the 30-gene signature overexpressed in GSCs. (B) Illustration of the results from protein network analysis of the 30-gene signature: the connections between the proteins (gray nodes and lines), coexpressed genes (pink lines), known physical interactions (blue lines) and predicted interactions (brown lines). White nodes are genes that are included in the network as they interact with many of the genes in the signature. (C) An expression index based on the summed z-scores of the GSC-upregulated genes correlates to an increasing grade of malignancy in glioma patients from Sun et al.

GSC signature using K-means clustering. In both datasets we identified a significant correlation between the GSC expression index and survival, with a median survival of 124 vs. 62 weeks (low and high signature, respectively) and 684 vs. 224 days (Fig. 4A & B and Table S4). For both datasets the two clusters included both WHO glioma grade III and GBM tumors. The fraction of grade IV tumors was higher in the group with high GSC expression signature; 85% vs. 60% and 97% vs. 64% in the two datasets (high and low signature, respectively). Interestingly, our GSC expression index showed a better ability to discern patient survival than a gene signature recently developed based on unsupervised gene clustering in the tumor bulk by Li et al. [30]; having a median survival of 97 vs. 65 weeks (low and high signature, respectively)

and 412 vs. 341 days (Table S4). This strongly suggests that our 30-gene signature is clinically relevant and provides evidence that the CSC model is applicable to human GBM.

Genes upregulated in GSCs correlate with the expression profiles of ESCs and iPSCs

To determine the extent to which the GSC signature is expressed across a wide range of cell types, a summary score was calculated for the expression of the GSC signature (5% FDR) across a large proportion of the publicly available gene expression arrays in the Gene Expression Omnibus ($\sim$160,000 arrays). Fitting the distribution of these scores to a mixture-model allowed for the calculation of a
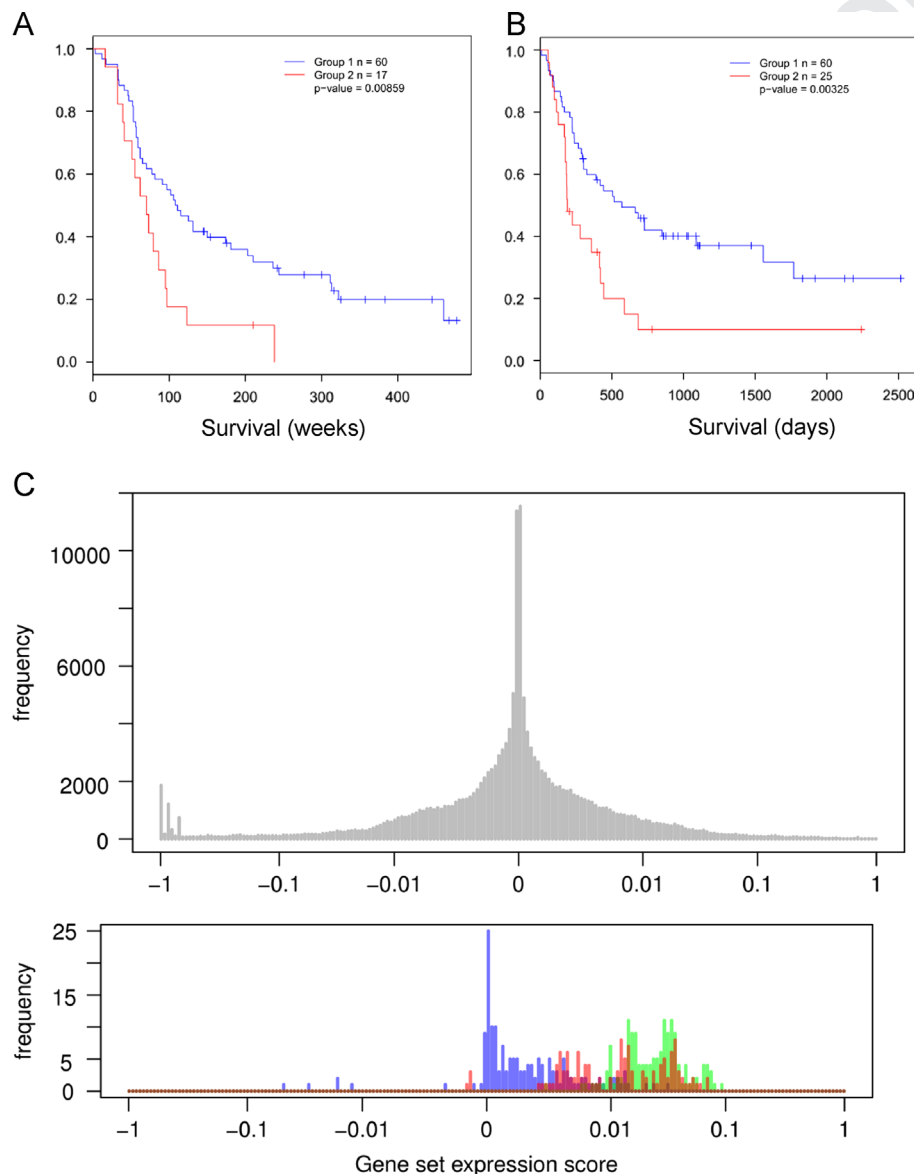
Fig. 4 – The enrichment of the GSC-upregulated signature correlates with decreased survival of glioma patients and pluripotency of ES/iPS cells. (A–B) Kaplan Meier plot of patients from the Phillips (A) and the Freije (B) datasets showing significantly decreased survival of glioma patients with a high expression of the 30-gene signature (group 2, red) (C) Upper histogram shows the normalized distribution of GSC up-regulated signature (5% FDR) across the GEO database corpus. Lower panel shows the increased expression of the GSC up-regulated signature (5% FDR) for a panel of 127 ESC (red) and 154 iPSC sources (green). A set of 127 fibroblasts was used as a control (blue).

probability of expression of the GSC signature in each array (Fig. 4C; upper panel). Within this dataset, a collection of embryonic stem cells (ESCs) and inducible pluripotent stem cells (iPSCs) arrays were manually curated to highlight the expression of the GSC signature in these arrays relative to the full GEO data. A set of fibroblast arrays was used as an additional control. The genes in the signature was found to be highly expressed within the group of 281 pluripotent arrays of ESCs and iPSCs ($p = 0.042$) (Fig. 4C; lower panel and Table S5), with a mean expression level higher than 96% of all arrays profiled. Calculated as individual groups, iPSCs ($p = 0.033$) showed a higher expression of this signature than ESCs ($p = 0.062$). These findings support the hypothesis that GSCs share gene expression programs with pluripotent cell types known for their tendency to generate tumors when transplanted in preclinical models of neuro-degenerative disease.

Dysregulation of pathways and networks in GSCs

The functional characteristics that distinguish GSCs from ahNSCs were determined by identifying signaling pathways and regulatory networks enriched in the differentially expressed gene signature. Two strategies were used, providing different levels of sensitivity and specificity. Firstly, using a differential gene expression analysis applying the Rank Product algorithm we identified 423 upregulated and 414 downregulated genes at 1% FDR (Fig. 1B and Table S6). The enrichment of canonical pathways in this gene list was determined using the hypergeometric distribution, based on pathways from the Kyoto Encyclopedia of Genes and Genomes (KEGG) and Wikipathways [41]. Twenty-four pathways were found to be significantly enriched (p-value < 0.01), with the cell cycle (p-value = 1.42E-13) and the Wnt pathway (p-value = 3.75E-5) being the most significant (Fig. 5 and Table S6).

Secondly we performed an additional analysis with a greater emphasis on sensitivity rather than specificity using the Comparative Marker Selection suite [16]. This identified 1713 upregulated and 2544 downregulated genes ($p < 0.05$) (Table S6). Their enrichment in the Canonical Pathways collections of the Molecular Signatures Database (MSigDB) were assessed by the hypergeometric distribution. The most significantly enriched upregulated

genes were related to the cell cycle (Cell Cycle Combined, DNA Replication Reactome, G1 To S1 Cell Cycle Reactome) and to cell signaling pathways (TNF, MAPK, NFKβ, mTOR, NOTCH and p53/apoptosis) (Fig. S2 and Table S6). Several pathways related to cell-to-cell interaction (Tight Junction, Axon guidance) and neuronal function (calcium regulation, GABA pathway) were downregulated in GSCs compared to their normal counterparts (Fig. S2 and Table S6).

Detailed information about the experiments and the resulting gene sets generated are available for pathway comparison with other stem and cancer and stem cell datasets in the online resource "The Stem Cell Discovery Engine" [20].

Stem cell pathways - the Wnt-pathway is more dysregulated than hedgehog and notch

Earlier studies have suggested that inhibition of the Hedgehog- or Notch-signaling pathway reduces the tumorigenicity of GSCs [7,11]. Interestingly, although we found that the Hedgehog pathway and activated transcriptional targets of the Notch pathway were enriched in GSCs ($p = 8.47 \times 10^{-4}$ and $p = 1.79 \times 10^{-3}$ respectively), the Wnt-signaling pathway was the most significantly dysregulated ($p = 3.75 \times 10^{-5}$). A gene-level analysis of each of these pathways and their downstream targets was conducted to provide a detailed understanding of their role in GSCs (Fig. 6).

Both cell types expressed very low levels of the Hedgehog pathway-associated Shh-ligand and the transcription factors GLI1 and GLI2. GSCs, however, expressed significantly higher levels of the membrane receptor smoothened (SMO) and the transcription factor GLI3 (Fig. 6). Significant upregulation of downstream targets ($p = 0.02$) supported the importance of the Hedgehog-pathway in GSCs.

The core genes necessary for Notch-signaling (KEGG) were present above background levels in both cell types. The Notch 2 receptor and the transcription factor Hes1 were significantly upregulated in GSCs (Fig. 6). Analysis of downstream targets gave ambiguous results as both activated and repressed targets of Notch were enriched in GSCs.
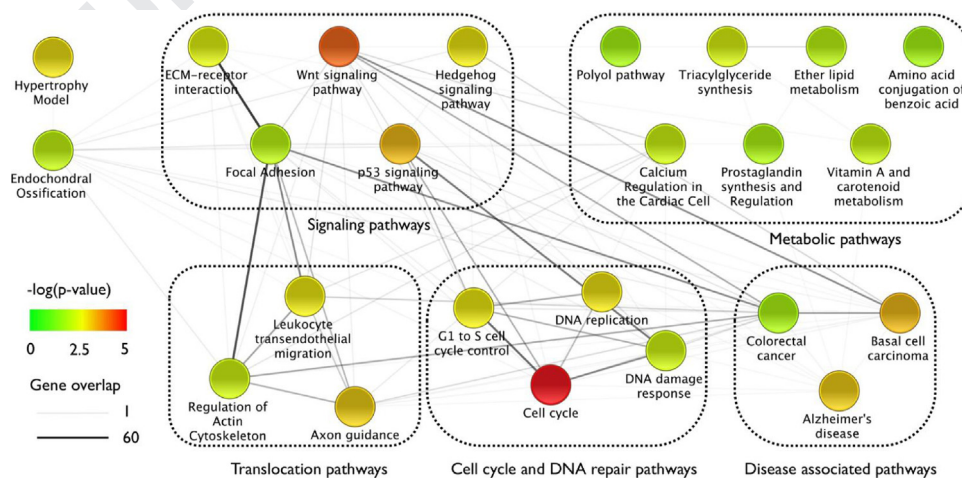
Fig. 5 – Network view of pathways being dysregulated in GSCs: The pathway analysis was based on the gene list identified by the Rank Product Algorithm (1% FDR) and was done using wikipathways and netpath. The significance of each pathway is reflected as indicated by the color code. Gene overlap between pathways is indicated by the intensity of the lines connecting the different pathways.
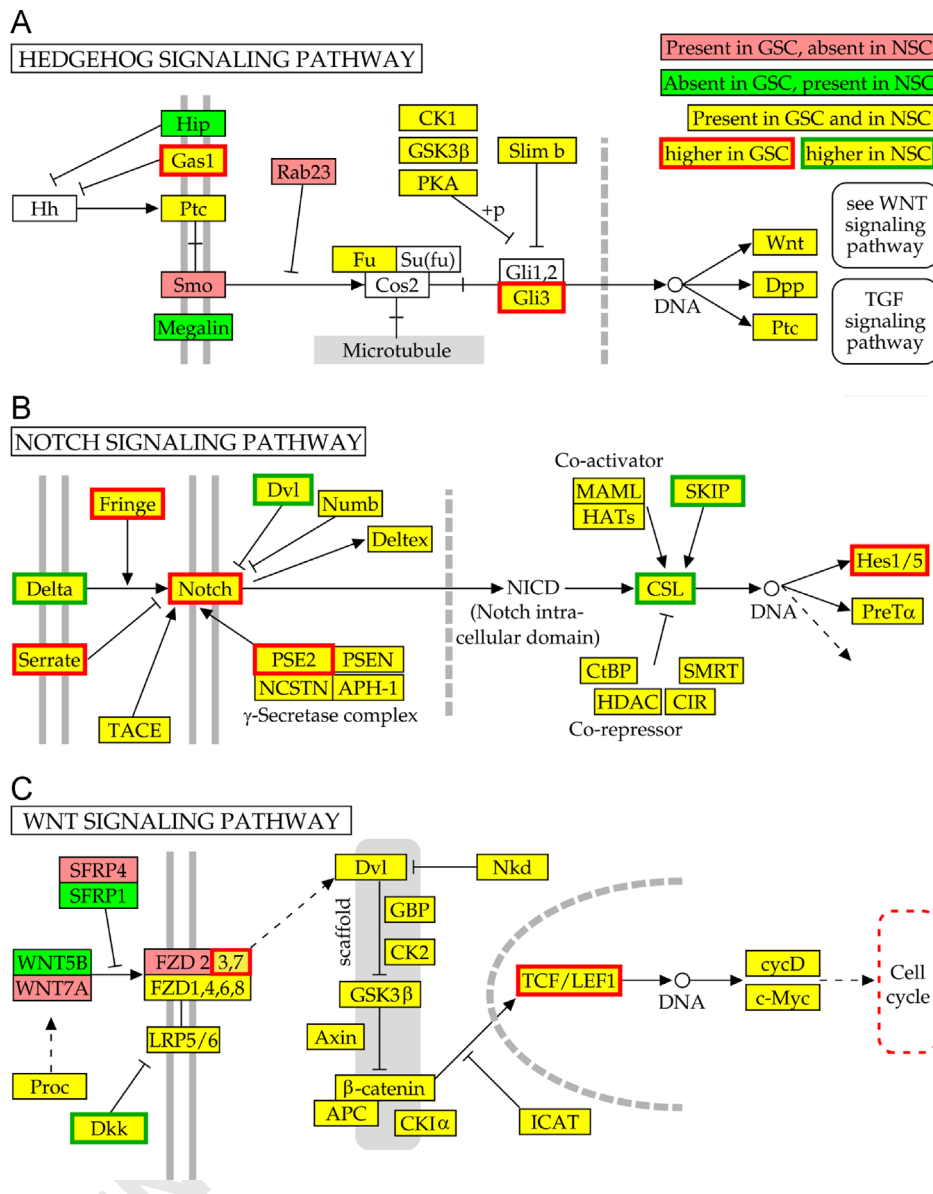
Fig. 6 – Pathway maps of gene expression data in Shh-, Notch- and Wnt-pathway: Pathway maps of the (A) Hedgehog-, (B) Notch- and (C) Wnt-signaling in GSCs compared to ahNSCs. Hedgehog- and Notch-pathway data were extracted from microarrays whereas Wnt data are from qPCR-analysis.

Analysis of the Wnt-pathway showed that core genes were expressed in both cell types, but a number of the pathway members were differentially regulated. The membrane receptors FZD3, 5 and 7 were upregulated in GSCs compared to ahNSCs, while soluble Frizzled related protein 1 (SFRP1) was significantly downregulated. The set of activated downstream targets of the Wnt pathway were also enriched in the set of GSC expressed genes ($p=0.002$).

Wnt-pathway dysregulation could be confirmed at gene expression- and protein level

To confirm the finding that the Wnt pathway plays a significant role in GBM/GSCs we performed a qPCR screen of more than 90 Wnt-related genes (Fig. 6 & supplementary Table S7). Excluding weakly expressed genes (Ct >30), we identified upregulation of WNT7A and FZD 2, 3 and 7 and downregulation of WNT5B. The

downregulation of SFRP1 and upregulation of SFRP4 was confirmed. LEF1 and TCL7F, transcription factors involved in Wnt downstream signaling, were significantly upregulated.

The activity of β-catenin depends on its phosphorylation state. In cells not exposed to Wnt signals, β-catenin levels are kept low as a result of phosphorylation by GSK-3. When cells are exposed to Wnt signals, GSK-3 is trapped in another complex and does not phosphorylate β-catenin anymore. Only this unphosphorylated, stabilized form of the protein can enter the nucleus to interact with transcription factors. To investigate the activity of β-catenin in GSCs and ahNSCs, we quantified both total and active (dephosphorylated) β-catenin by western blot. While total β-catenin was present in both cell types, its active form was only present in GSCs (Fig. 7E). To further establish the activation status of Wnt-signaling in GSCs, we used immunofluorescence combined with confocal microscopy to determine the subcellular localization of
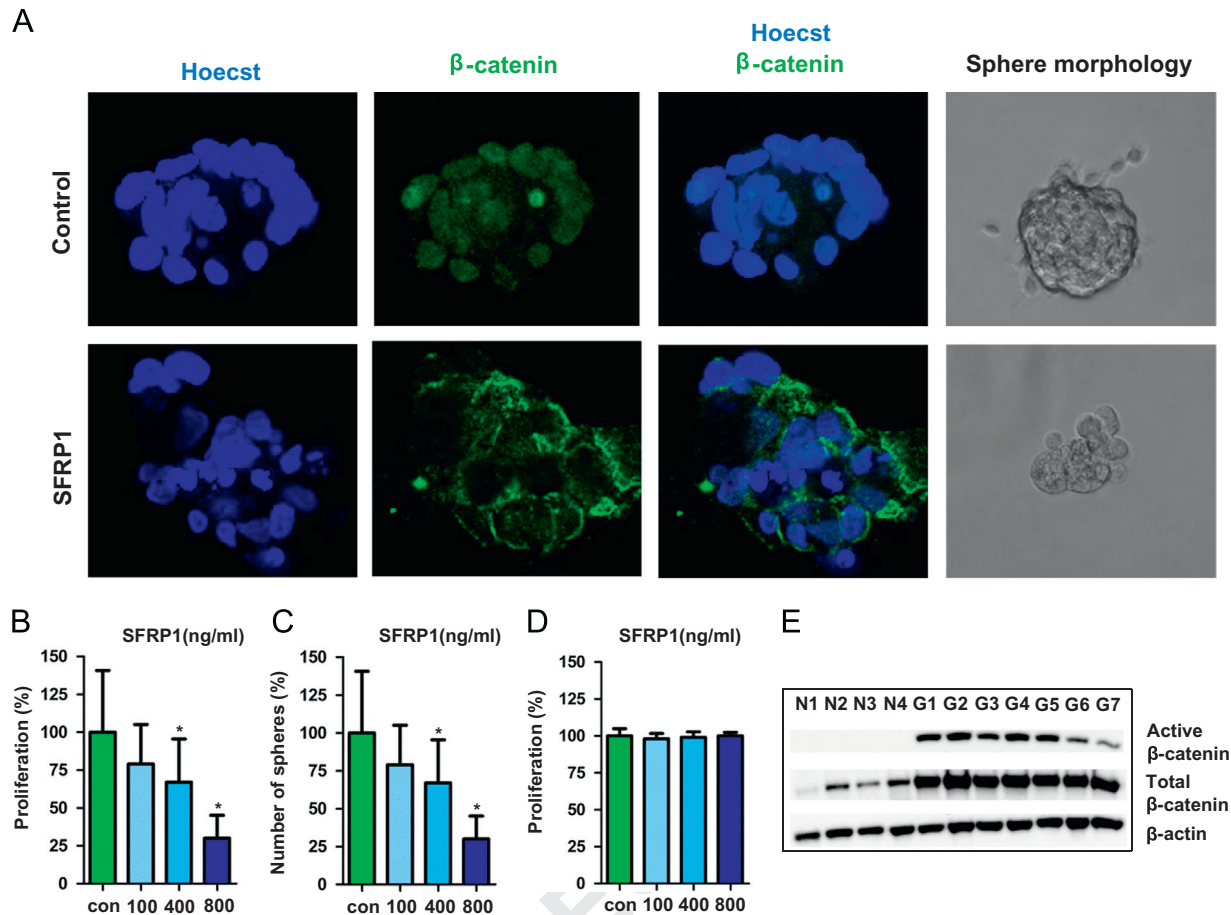
Fig. 7 – β-Catenin is highly upregulated in GSCs and SFRP1 regulates their proliferation and sphere forming capacity:
(A) Immunofluoresence of spheres showing the expression of active β-catenin (green) in non-treated GSCs (upper panel) and SFRP1 treated GSCs (3200 ng/ml, lower panel). Cell nuclei were stained with Hoechst (blue). SFRP1 treated spheres display altered sphere morphology compared to controls. (B) SFRP1 treatment reduces cell proliferation dose-dependently in GSCs. Results are presented as mean$\pm$SD of three individual experiments and calculated as percentage of controls. Bars with * have p-value < 0.01 (C) SFRP1 treatment reduces sphere formation dose-dependently in GSCs. Results are presented as mean$\pm$SD of three individual experiments and calculated as percentage of controls. Bars with * have p-value < 0.01 (D) SFRP1 treatment does not reduce cell proliferation in ahNSCs. Results are presented as mean$\pm$SD of three individual experiments and calculated as percentage of controls (E) Western blot showing the differential protein expression of active β-catenin and total β-catenin between ahNSCs (N) and GSCs (G). β-Actin was used as a loading control.

β-catenin. This showed the presence of active β-catenin in the nucleus of GSCs (Fig. 7A, upper panel). These data further support the finding that Wnt-signaling is upregulated in GSCs.

Wnt-pathway inhibition reduces proliferation and sphere forming capacity in GSCs

GSCs proliferate and form spheres much more efficiently than ahNSCs [49], and the ability to form such spheres is a prognostic predictor for patients with GBM [27]. Our data indicated both downregulation of the naturally occurring Wnt antagonist SFRP1 and an upregulation of Wnt pathway ligands, receptors and transcription factors in GSCs. Therefore, we investigated the effect of SFRP1 on GSCs and ahNSCs in culture. Recombinant SFRP1 was added daily in three different concentrations to the GSC and ahNSC cultures for two weeks. This treatment led to a significant and dose-dependent reduction of both proliferation and sphere formation in GSCs by as much as 70% and 50%, respectively (Fig. 7B & C). In contrast, SFRP1-stimulation did not interfere with proliferation of ahNSC (Fig. 7D). SFRP1 treated spheres were also smaller than non-treated (Fig. 7A, right) and β-catenin was located in the cytoplasm and the cell membrane, instead of in the nucleus (Fig. 7A, lower panel). This indicates that loss of naturally occurring Wnt-inhibition through downregulation of SFRP1 is important for GSCs' ability to proliferate and self-renew.

Discussion

We have developed the first internally consistent experimental and molecular reference between GSCs and ahNSCs using functionally validated sphere-forming cells. Sphere-forming conditions enriched

for stem cells but result in a heterogeneous mixture of stem- and progenitor cells. There is, however, evidence that comparison of closely related but distinguishable cell fractions can reveal stem cell specific gene expression, even though the actual stem cell frequency is relatively low. For example, many genes identified from enriched but not purified HSC fractions have subsequently been shown to have HSC-specific function [15,39]. Similarly, in this study we identified MELK and EHZ2, both of which have earlier been suggested to regulate GSC self-renewal and tumor initiating capacity [37,38,46]. Our strategy of directly comparing expression patterns of GSCs to ahNSCs, as opposed to non-stem cell populations, has enhanced our ability to identify genes and pathways that are disrupted at the stem cell level in GBM.

While there is substantial preclinical evidence that certain cancers are organized in cell hierarchies initiated and maintained by a CSC, the relevance of this model in human disease is still uncertain. Two independent groups compared transcriptional programs of functionally validated LSCs and HSCs, identified a LSC gene signature, and showed that high expression of this signature was associated with adverse clinical outcome in human leukemia [9,14]. These studies were first to provide substantial support for the CSC hypothesis in leukemia from a clinical perspective. Using a similar strategy we have here identified a gene expression signature that exists in GSCs, but not in ahNSCs, that correlates to survival in independent data sets. This indicates that GSCs are of clinical importance in GBM.

Recently, Engström et al. compared four glioma stem cell lines with two human fetal neural lines [8]. In contrast to both our study and the study of Majeti et al. on LSCs, both of which used early passage normal stem cells from relevant normal human tissue, Engström el al. used cells that were (1) fetal and (2) grown as adherent cell lines [32]. This result in a different cell type and accordingly, a very different profile from what we found when comparing GSCs to ahNSCs. While Engström et al. identified 739 genes being differentially regulated within a significance level of 10% FDR, a similar cut-off in our study generated a list of 3264 differentially regulated genes. The two lists had 247 genes in common, but none of these were among our most significant genes (179 genes, FDR 0.1%). Consequently, the extracted core signatures capturing the major gene expression alterations in the respective studies differ. This was also reflected in the results from pathway analysis identifying the top-most enriched KEGG-pathways. While our study identified the cell cycle and the Wnt pathway, Engström et al. identified cytokine–cytokine receptor interaction and the chemokine signaling pathway as the most dysregulated pathways. ECM-receptor interaction was the only pathway shared between the two studies. Despite differences in the cell types used and the signatures identified, the results from Engström et al. are in consistent with a clinical relevance of the CSC hypothesis in solid tumors.

We found that GSC cultures were more heterogeneous than ahNSCs. While our GSC cultures covered a spectrum of TCGA subtypes, all five ahNSCs correlated with the neural subtype. Not all GSC cultures showed enrichment of a particular subgroup. The TCGA sub-classification [50] was, however, developed using tumor bulk tissue and may not be optimal for stem cell enriched cell types. Although significant, the expression scores of subtype-genes in GSCs were not as high as those found in tissue samples. Subtyping of the samples according to Lottaz et al. identified one sample (G9) as their type I with a mesenchymal profile similar to ahNSCs. G9 was also identified as mesenchymal according to TCGA. Lottaz showed that their type II corresponds with a proneural phenotype, but did not investigate enrichment of subtypes other than mesenchymal and proneural. Our samples identified as Lottaz type II, were enriched in genes of either the proneural or classical TCGA subtypes. In order to get a full overview of the tumor initiating cell/stem cell population and significantly establish subtypes of GSCs, it will be important to cultivate cells from a larger number of patients.

We also found that genes up-regulated in GSCs were highly expressed in both ESCs and iPSCs as compared to the other arrays in the GEO database. This is in keeping with the tendency of these cell types to form tumors following transplantation in preclinical models of neurodegenerative disease repair [4]. The identified correlation of GSCs with iPSCs was higher than the correlation of GSCs with ESCs, supporting recent literature indicating that iPSCs are likely to be more tumorigenic than ESCs [2].

Pathway analysis identified that GSCs express a gene signature typically associated with migrating cells and the interaction of stem cells with their niche: axon guidance, adherens junction, focal adhesion, regulation of actin cytoskeleton and leukocyte trans-endothelial migration. With the exception of axon guidance, these pathways were also identified as the top-most dysregulated pathways in leukemic cells in the only other study directly comparing cancer stem cells to somatic adult stem cells [33]. Thus, CSCs of different origin may have common features. A growing number of studies on stem cell related cancers are being performed. It is important to be able to determine the underlying molecular phenotype of CSCs, in particular, to determine if there are common molecular events between cancer stem cell studies. To facilitate such comparisons, we have made the data generated by this study available within a specialized resource for stem- and cancer stem cell signatures that is structured to facilitate discovery of common and unique pathway utilization between signatures [20].

The Wnt- and Hedgehog-pathway genes, as well as Notch-regulated targets showed altered expression in GSCs. These three pathways are important regulators of adult NSCs [1,26,31], and Hedgehog- and Notch- signaling have additionally been suggested to be involved in regulating GSCs [7,11]. Here, we have identified and characterized canonical Wnt-pathway dysregulation in GSCs.

Within the Wnt-pathway we identified significant downregulation of SFRP1 and upregulation of FZD receptors (FZD 2, 3 and 7) in GSCs. Active β-catenin was only present in GSCs. A primary trait of GSCs is that they form spheres and proliferate much more efficiently than ahNSCs [49]. This ability to form spheres corre-lates with clinical outcome [27]. We found that re-establishing SFRP1-inhibition in GSCs decreases both proliferation and sphere forming ability. In contrast, SFRP1-stimulation did not interfere with proliferation of ahNSCs. These findings are in keeping with effects observed earlier in normal HSCs [36] and ESCs [23].

Our study provides evidence substantiating the clinical rele-vance of CSCs in solid tumors and gives critical insights into the similarities and differences between adult normal and malignant stem cell populations. The results may be used for the develop-ment of targeted therapies and as tools for assessing the impact of therapy on the GSC population.

Financial support

Conflicts of interest

None.

Acknowledgments

Appendix A.   Supporting information

Supplementary data associated with this article can be found in the online version at http://dx.doi.org/10.1016/j.yexcr.2013.06.004.

REFERENCES

[1] A. Androutsellis-Theotokis, R.R. Leker, F. Soldner, D.J. Hoeppner, R. Ravin, S.W. Poser, M.A. Rueger, S.K. Bae, R. Kittappa, R.D. McKay, et al., Notch signalling regulates stem cell numbers in vitro and in vivo, Nature 442 (2006) 823–826.

[2] U. Ben-David, N. Benvenisty, et al., The tumorigenicity of human embryonic and induced pluripotent stem cells, Nat. Rev. Cancer 11 (2011) 268–277.

[3] D. Bonnet, J.E. Dick, et al., Human acute myeloid leukemia is organized as a hierarchy that originates from a primitive hematopoietic cell, Nat. Med. 3 (1997) 730–737.

[4] A. Brederlau, A.S. Correia, S.V. Anisimov, M. Elmi, G. Paul, L. Roybon, A. Morizane, F. Bergquist, I. Riebe, U. Nannmark, M. Carta, E. Hanse, J. Takahashi, Y. Sasai, K. Funa, P. Brundin, P.S. Eriksson, J.Y. Li, et al., Transplantation of human embryonic stem cell-derived cells to a rat model of Parkinson's disease: effect of in vitro differentiation on graft survival and teratoma formation, Stem Cells 24 (2006) 1433–1440.

[5] R. Breitling, P. Armengaud, A. Amtmann, P. Herzyk, et al., Rank products: a simple, yet powerful, new method to detect differentially regulated genes in replicated microarray experiments, FEBS Lett. 573 (2004) 83–92.

[6] R. Chen, M.C. Nishimura, S.M. Bumbaca, S. Kharbanda, W.F. Forrest, I.M. Kasman, J.M. Greve, R.H. Soriano, L.L. Gilmour, C.S. Rivers, Z. Modrusan, S. Nacu, S. Guerrero, K.A. Edgar, J.J. Wallin, K. Lamszus, M. Westphal, S. Heim, C.D. James, S.R. VandenBerg, J.F. Costello, S. Moorefield, C.J. Cowdrey, M. Prados, H.S. Phillips, et al., A hierarchy of self-renewing tumor-initiating cell types in glioblastoma, Cancer Cell 17 (2010) 362–375.

[7] V. Clement, P. Sanchez, T.N. de, I. Radovanovic, A. Altaba, et al., HEDGEHOG-GLI1 signaling regulates human glioma growth, cancer stem cell self-renewal, and tumorigenicity, Curr. Biol. 17 (2007) 165–172.

[8] P.G. Engstrom, D. Tommei, S.H. Stricker, C. Ender, S.M. Pollard, P. Bertone, et al., Digital transcriptome profiling of normal and glioblastoma-derived neural stem cells identifies genes associated with patient survival, Genome Med. 4 (2012) 76.

[9] K. Eppert, K. Takenaka, E.R. Lechman, L. Waldron, B. Nilsson, G.P. van, K.H. Metzeler, A. Poeppl, V. Ling, J. Beyene, A.J. Canty, J.S. Danska, S.K. Bohlander, C. Buske, M.D. Minden, T.R. Golub, I. Jurisica, B.L. Ebert, J.E. Dick, et al., Stem cell gene expression programs influence clinical outcome in human leukemia, Nat. Med. 17 (2011) 1086–1093.

[10] A. Ernst, S. Hofmann, R. Ahmadi, N. Becker, A. Korshunov, F. Engel, C. Hartmann, J. Felsberg, M. Sabel, H. Peterziel, M. Durchdewald, J. Hess, S. Barbus, B. Campos, A. Starzinski-Powitz, A. Unterberg, G. Reifenberger, P. Lichter, C. Herold-Mende, B. Radlwimmer, et al., Genomic and expression profiling of glioblastoma stem cell-like spheroid cultures identifies novel tumor-relevant genes associated with survival, Clin. Cancer Res. 15 (2009) 6541–6550.

[11] X. Fan, L. Khaki, T.S. Zhu, M.E. Soules, C.E. Talsma, N. Gul, C. Koh, J. Zhang, Y.M. Li, J. Maciaczyk, G. Nikkhah, F. Dimeco, S. Piccirillo, A.L. Vescovi, C.G. Eberhart, et al., NOTCH pathway blockade depletes CD133-positive glioblastoma cells and inhibits growth of tumor neurospheres and xenografts, Stem Cells 28 (2010) 5–16.

[12] W.A. Freije, F.E. Castro-Vargas, Z. Fang, S. Horvath, T. Cloughesy, L.M. Liau, P.S. Mischel, S.F. Nelson, et al., Gene expression profiling of gliomas strongly predicts survival, Cancer Res. 64 (2004) 6503–6510.

[13] A.J. Gentles, S.K. Plevritis, R. Majeti, A.A. Alizadeh, et al., Association of a leukemic stem cell gene expression signature with clinical outcomes in acute myeloid leukemia, JAMA 304 (2010) 2706–2715.

[14] A.J. Gentles, S.K. Plevritis, R. Majeti, A.A. Alizadeh, et al., Association of a leukemic stem cell gene expression signature with clinical outcomes in acute myeloid leukemia, JAMA 304 (2010) 2706–2715.

[15] R.W. Georgantas III, V. Tanadve, M. Malehorn, S. Heimfeld, C. Chen, L. Carr, F. Martinez-Murillo, G. Riggins, J. Kowalski, C.I. Civin, et al., Microarray and serial analysis of gene expression analyses identify known and novel transcripts overexpressed in hematopoietic stem cells, Cancer Res. 64 (2004) 4434–4441.

[16] J. Gould, G. Getz, S. Monti, M. Reich, J.P. Mesirov, et al., Comparative gene marker selection suite, Bioinformatics 22 (2006) 1924–1925.

[17] H.S. Gunther, N.O. Schmidt, H.S. Phillips, D. Kemming, S. Kharbanda, R. Soriano, Z. Modrusan, H. Meissner, M. Westphal, K. Lamszus, et al., Glioblastoma-derived stem cell-enriched cultures form distinct subgroups according to molecular and phenotypic criteria, Oncogene 27 (2008) 2897–2909.

[18] R. Helseth, E. Helseth, T.B. Johannesen, C.W. Langberg, K. Lote, P. Ronning, D. Scheie, A. Vik, T.R. Meling, et al., Overall survival, prognostic factors, and repeated surgery in a consecutive series of 516 patients with glioblastoma multiforme, Acta Neurol. Scand. 122 (2010) 159–167.

[19] S.J. Ho Sui, K. Begley, D. Reilly, B. Chapman, R. McGovern, P. Rocca-Sera, E. Maguire, G.M. Altschuler, T.A. Hansen, R. Sompallae, A. Krivtsov, R.A. Shivdasani, S.A. Armstrong, A.C. Culhane, M. Correll, S.A. Sansone, O. Hofmann, W. Hide, et al., The Stem Cell discovery engine: an integrated repository and analysis system for cancer stem cell comparisons, Nucleic Acids Res. 40 (2012) D984–D991.

[20] S.J. Ho Sui, K. Begley, D. Reilly, B. Chapman, R. McGovern, P. Rocca-Sera, E. Maguire, G.M. Altschuler, T.A. Hansen, R. Sompallae, A. Krivtsov, R.A. Shivdasani, S.A. Armstrong, A.C. Culhane, M. Correll, S.A. Sansone, O. Hofmann, W. Hide, et al., The Stem Cell discovery engine: an integrated repository and analysis system for cancer stem cell comparisons, Nucleic Acids Res. 40 (2012) D984–D991.

[21] T.N. Ignatova, V.G. Kukekov, E.D. Laywell, O.N. Suslov, F.D. Vrionis, D.A. Steindler, et al., Human cortical glial tumors contain neural stem-like cells expressing astroglial and neuronal markers in vitro, Glia 39 (2002) 193–206.

[22] C.B. Johansson, M. Svensson, L. Wallstedt, A.M. Janson, J. Frisen, et al., Neural stem cells in the adult human brain, Exp. Cell Res. 253 (1999) 733–736.

[23] M.B. Jones, C.H. Chu, J.C. Pendleton, M.J. Betenbaugh, B. Baljinnyam, J.S. Rubin, M.J. Shamblott, et al., Proliferation and pluripotency of human embryonic stem cells maintained on type I collagen, Stem Cells Dev. 19 (2010) 1923–1935.

[24] W. Kim, L.M. Liau, et al., IDH mutations in human glioma, Neurosurg. Clin. N. Am 23 (2012) 471–480.

Q2 [25] W.K. Kleihus, et al., PC Pathology and Genetics: Tumors of the Nervous System, , 2000.

[26] K. Lai, B.K. Kaspar, F.H. Gage, D.V. Schaffer, et al., Sonic hedgehog regulates adult neural progenitor proliferation in vitro and in vivo, Nat. Neurosci. 6 (2003) 21–27.

[27] D.R. Laks, M. Masterman-Smith, K. Visnyei, B. Angenieux, N.M. Orozco, I. Foran, W.H. Yong, H.V. Vinters, L.M. Liau, J.A. Lazareff, P. S. Mischel, T.F. Cloughesy, S. Horvath, H.I. Kornblum, et al., Neurosphere formation is an independent predictor of clinical outcome in malignant glioma, Stem Cells 27 (2009) 980–987.

[28] T. Lapidot, C. Sirard, J. Vormoor, B. Murdoch, T. Hoang, J. Caceres-Cortes, M. Minden, B. Paterson, M.A. Caligiuri, J.E. Dick, et al., A cell initiating human acute myeloid leukaemia after transplantation into SCID mice, Nature 367 (1994) 645–648.

[29] J. Lee, S. Kotliarova, Y. Kotliarov, A. Li, Q. Su, N.M. Donin, S. Pastorino, B.W. Purow, N. Christopher, W. Zhang, J.K. Park, H.A. Fine, et al., Tumor stem cells derived from glioblastomas cultured in bFGF and EGF more closely mirror the phenotype and genotype of primary tumors than do serum-cultured cell lines, Cancer Cell 9 (2006) 391–403.

[30] A. Li, J. Walling, S. Ahn, Y. Kotliarov, Q. Su, M. Quezado, J.C. Oberholtzer, J. Park, J.C. Zenklusen, H.A. Fine, et al., Unsupervised analysis of transcriptomic profiles reveals six glioma subtypes, Cancer Res. 69 (2009) 2091–2099.

[31] D.C. Lie, S.A. Colamarino, H.J. Song, L. Desire, H. Mira, A. Consiglio, E.S. Lein, S. Jessberger, H. Lansford, A.R. Dearie, F.H. Gage, et al., Wnt signalling regulates adult hippocampal neurogenesis, Nature 437 (2005) 1370–1375.

[32] C. Lottaz, D. Beier, K. Meyer, P. Kumar, A. Hermann, J. Schwarz, M. Junker, P.J. Oefner, U. Bogdahn, J. Wischhusen, R. Spang, A. Storch, C.P. Beier, et al., Transcriptional profiles of CD133+ and C, Cancer Res. 70 (2010) 2030–2040.

[33] R. Majeti, M.W. Becker, Q. Tian, T.L. Lee, X. Yan, R. Liu, J.H. Chiang, L. Hood, M.F. Clarke, I.L. Weissman, et al., Dysregulated gene expression networks in human acute myelogenous leukemia stem cells, Proc. Natl. Acad. Sci. U.S.A 106 (2009) 3396–3401.

[34] M.C. Moe, M. Varghese, A.I. Danilov, U. Westerlund, J. Ramm-Pettersen, L. Brundin, M. Svensson, J. Berg-Johnsen, I.A. Langmoen, et al., Multipotent progenitor cells from the adult human brain: neurophysiological differentiation to mature neurons, Brain 128 (2005) 2189–2199.

[35] M.C. Moe, U. Westerlund, M. Varghese, J. Berg-Johnsen, M. Svensson, I.A. Langmoen, et al., Development of neuronal networks from single stem cells harvested from the adult human brain, Neurosurgery 56 (2005) 1182–1188.

[36] H. Nakajima, M. Ito, Y. Morikawa, T. Komori, Y. Fukuchi, F. Shibata, S. Okamoto, T. Kitamura, et al., Wnt modulators, SFRP-1, and SFRP-2 are expressed in osteoblasts and differentially regulate hematopoietic stem cells, Biochem. Biophys. Res. Commun. 390 (2009) 65–70.

[37] I. Nakano, M. Masterman-Smith, K. Saigusa, A.A. Paucar, S. Horvath, L. Shoemaker, M. Watanabe, A. Negro, R. Bajpai, A. Howes, V. Lelievre, J.A. Waschek, J.A. Lazareff, W.A. Freije, L.M. Liau, R.J. Gilbertson, T.F. Cloughesy, D.H. Geschwind, S.F. Nelson, P.S. Mischel, A.V. Terskikh, H.I. Kornblum, et al., Maternal embryonic leucine zipper kinase is a key regulator of the proliferation of malignant brain tumors, including brain tumor stem cells, J. Neurosci. Res. 86 (2008) 48–60.

[38] I. Nakano, A.A. Paucar, R. Bajpai, J.D. Dougherty, A. Zewail, T.K. Kelly, K.J. Kim, J. Ou, M. Groszer, T. Imura, W.A. Freije, S.F. Nelson, M.V. Sofroniew, H. Wu, X. Liu, A.V. Terskikh, D.H. Geschwind, H.I. Kornblum, et al., Maternal embryonic leucine zipper kinase (MELK) regulates multipotent neural progenitor proliferation, J. Cell Biol. 170 (2005) 413–427.

[39] F. Notta, S. Doulatov, E. Laurenti, A. Poeppl, I. Jurisica, J.E. Dick, et al., Isolation of single human hematopoietic stem cells capable of long-term multilineage engraftment, Science 333 (2011) 218–221.

[40] H.S. Phillips, S. Kharbanda, R. Chen, W.F. Forrest, R.H. Soriano, T.D. Wu, A. Misra, J.M. Nigro, H. Colman, L. Soroceanu, P.M. Williams, Z. Modrusan, B.G. Feuerstein, K. Aldape, et al., Molecular subclasses of high-grade glioma predict prognosis, delineate a pattern of disease progression, and resemble stages in neurogenesis, Cancer Cell 9 (2006) 157–173.

[41] A.R. Pico, T. Kelder, M.P. van Iersel, K. Hanspers, B.R. Conklin, C. Evelo, et al., WikiPathways: pathway editing for the people, PLoS. Biol. 6 (2008) e184.

[42] L. Prestegarden, A. Svendsen, J. Wang, L. Sleire, K.O. Skaftnesmo, R. Bjerkvig, T. Yan, L. Askland, A. Persson, P.O. Sakariassen, P.O. Enger, et al., Glioma cell populations grouped by different cell type markers drive brain tumor growth, Cancer Res. 70 (2010) 4274–4279.

[43] M. Rahman, L. Deleyrolle, V. Vedam-Mai, H. Azari, M. Abd-El-Barr, B.A. Reynolds, et al., The cancer stem cell hypothesis: failures and pitfalls, Neurosurgery 68 (2011) 531–545.

[44] B.A. Reynolds, S. Weiss, et al., Generation of neurons and astrocytes from isolated cells of the adult mammalian central nervous system, Science 255 (1992) 1707–1710.

[45] L. Sun, A.M. Hui, Q. Su, A. Vortmeyer, Y. Kotliarov, S. Pastorino, A. Passaniti, J. Menon, J. Walling, R. Bailey, M. Rosenblum, T. Mikkelsen, H.A. Fine, et al., Neuronal and glioma-derived stem cell factor induces angiogenesis within the brain, Cancer Cell 9 (2006) 287–300.

[46] M.L. Suva, N. Riggi, M. Janiszewska, I. Radovanovic, P. Provero, J.C. Stehle, K. Baumer, M.A. Le Bitoux, D. Marino, L. Cironi, V.E. Marquez, V. Clement, I. Stamenkovic, et al., EZH2 is essential for glioblastoma cancer stem cell maintenance, Cancer Res. 69 (2009) 9211–9218.

[47] D.C. Taussig, F. Miraki-Moud, F. Anjos-Afonso, D.J. Pearce, K. Allen, C. Ridler, D. Lillington, H. Oakervee, J. Cavenagh, S.G. Agrawal, T.A. Lister, J.G. Gribben, D. Bonnet, et al., Anti-CD38 antibody-mediated clearance of human repopulating cells masks the heterogeneity of leukemia-initiating cells, Blood 112 (2008) 568–575.

[48] D.C. Taussig, J. Vargaftig, F. Miraki-Moud, E. Griessinger, K. Sharrock, T. Luke, D. Lillington, H. Oakervee, J. Cavenagh, S.G. Agrawal, T.A. Lister, J.G. Gribben, D. Bonnet, et al., Leukemia-initiating cells from some acute myeloid leukemia patients with mutated nucleophosmin reside in the CD34(-) fraction, Blood 115 (2010) 1976–1984.

[49] M. Varghese, H. Olstorn, C. Sandberg, E.O. Vik-Mo, P. Noordhuis, M. Nister, J. Berg-Johnsen, M.C. Moe, I.A. Langmoen, et al., A comparison between stem cells from the adult human brain and from brain tumors, Neurosurgery 63 (2008) 1022–1033.

[50] R.G. Verhaak, K.A. Hoadley, E. Purdom, V. Wang, Y. Qi, M.D. Wilkerson, C.R. Miller, L. Ding, T. Golub, J.P. Mesirov, G. Alexe, M. Lawrence, M. O'Kelly, P. Tamayo, B.A. Weir, S. Gabriel, W. Winckler, S. Gupta, L. Jakkula, H.S. Feiler, J.G. Hodgson, C.D. James, J.N. Sarkaria, C. Brennan, A. Kahn, P.T. Spellman, R.K. Wilson, T.P. Speed, J.W. Gray, M. Meyerson, G. Getz, C.M. Perou, D.N. Hayes, et al., Integrated genomic analysis identifies clinically relevant subtypes of glioblastoma characterized by abnormalities in PDGFRA, IDH1, EGFR, and NF1, Cancer Cell 17 (2010) 98–110.

[51] E.O. Vik-Mo, C. Sandberg, H. Olstorn, M. Varghese, P. Brandal, J. Ramm-Pettersen, W. Murrell, I.A. Langmoen, et al., Brain tumor stem cells maintain overall phenotype and tumorigenicity after in vitro culturing in serum-free conditions, Neuro. Oncol. 12 (2010) 1220–1230.

[52] J. Wang, P.O. Sakariassen, O. Tsinkalovsky, H. Immervoll, S.O. Boe, A. Svendsen, L. Prestegarden, G. Rosland, F. Thorsen, L. Stuhr,

A. Molven, R. Bjerkvig, P.O. Enger, et al., CD133 negative glioma cells form tumors in nude rats and give rise to CD133 positive cells, Int. J. Cancer 122 (2008) 761–768.

[53] D. Warde-Farley, S.L. Donaldson, O. Comes, K. Zuberi, R. Badrawi, P. Chao, M. Franz, C. Grouios, F. Kazi, C.T. Lopes, A. Maitland, S. Mostafavi, J. Montojo, Q. Shao, G. Wright, G.D. Bader, Q. Morris, et al., The GeneMANIA prediction server: biological network integration for gene prioritization and predicting gene function, Nucleic Acids Res. 38 (2010) W214–W220.